Journal of Modern Technology and Engineering
Vol.6, No.2, 2021, pp.124-142

FEEDBACK LINEARIZATION BASED ADAPTIVE STABILIZING CONTROLLER DESIGN COUPLED WITH FUZZY LOGIC SWING-UP FOR PENDULUM ON A CART

Daniel Abebe[1*], **Dr. Dereje Shiferaw**[2]

[1]Debre Berhan University, Debre Berhan, Ethiopia
[2]Addis Ababa Institute of Technology, Addis Ababa, Ethiopia

Abstract. This paper address an adaptive stabilizing controller for inverted pendulum on a cart based on feedback linearization coupled with an adaptive fuzzy logic based swing up controller. First feedback linearizing control signal is derived by decomposing the system into cart subsystem and pendulum subsystem. Then adaptive inverse control technique will be applied to each feedback linearizing control signals. An adaptive inverse control method is used for compensation of unknown parameters of an inverted pendulum on a cart, while feedback linearization is used to cancel non-linearity in the system. The pendulum will be driven from it's pendant position to inverted position using an adaptive fuzzy logic based swing up controller. When the pendulum reaches near it's inverted position, the stabilizing controller takes over the swing up controller. The MATLAB/SIMULINK simulation shows that the proposed controllers adapt to unknown mass of a cart between $0.1kg$ - $4kg$ and mass of a pendulum between $0.01kg$ - $4kg$.

Keywords: Feedback linearization, adaptive inverse control, fuzzy logic, swing up, IPC.
AMS Subject Classification: 93C42; 93C40; 93C10; 70Q05.
Corresponding author: Daniel Abebe, Debre Berhan University, Debre Berhan, Ethiopia, Tel.: +251920676932, e-mail: *abebe.daniel7@gmail.com*
Received: 18 February 2021; Revised: 30 April 2021; Accepted: 13 June 2021; Published: 31 August 2021.

1 Introduction

The inverted pendulum on a cart indicated on Figure 1 is a popular benchmark problem for researchers in control systems and automation. It is also a very good platform to verify and apply different control logic's in the field of control theory (Ogata & Yang, 2002). The pendulum is stable while hanging downwards, but the inverted pendulum is inherently unstable nonlinear system and needs to be balanced. Stabilizing controller for inverted pendulum can be linear model based classical linear controllers or non linear controllers. Nonlinear controller design methods take non-linearity in dynamic system into consideration during designing controller for the dynamic system. There are many controllers designed using this method for stabilization of inverted pendulum on a cart. The authors of Chen & Chen (1998) design adaptive sliding mode controller for inverted pendulum using fuzzy logic based reference model. While authors of Park & Chwa (2009) design coupled sliding-mode control (SMC) for inverted-pendulum systems.

There is also neural network based controller as on Mladenov et al. (2009), which decouples the system into position control and angle control and uses neural network based PID controller to stabilize inverted pendulum on a cart. Fuzzy controller for stabilization of inverted pendulum on a cart Sankaran (2008), Wu & Wang (2011) and adaptive fuzzy controller are also used in stabilizing and swing up of an inverted pendulum based on feedback linearization (El-Hawwary et al., 2006).

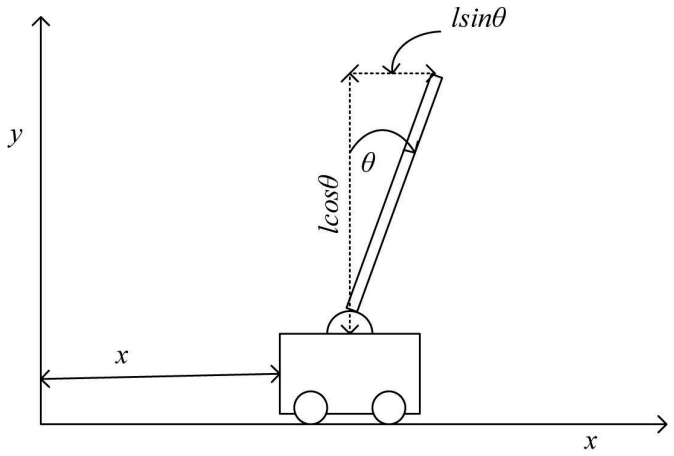

Figure 1: Inverted pendulum on a cart

Since the dynamics of an inverted pendulum on a cart in not involutive, exact input state feedback linearization is impossible. Thus some researchers use approximated feedback linearization to design stabilizing controller (Garcia-Chavez & Munoz-Panduro, 2017; Pathak, 2005; Renou & Saydy, 1996). Computed feedback linearization based controller is also used as indicated on Chanchareon (2006) for position tracking problem and regulation of inverted pendulum on a cart. While the authors of James (2015) used input-output feedback linearization in combination with sliding mode control and energy based swing up. Authors of Yakoub (2013) has designed feedback linearization combined with back-stepping for stabilization of inverted pendulum on a cart.

Recently researchers applied the concept of feedback linearization to design controller for dynamic systems like magnetic levitation Torres (2012), induction machine control Jeon & Choi (2000) and Magnetic Telemanipulation Shameli et al. (2008).

Swinging the pendulum from pendant position to an inverted position is an other interesting problem. Instead of driving it manually, researchers develop different methods to solve this particular problem. Energy based methods can be designed based on the energy of the whole system or only the energy of the pendulum (Yoshida, 1999; Åström & Furuta, 2000). These methods can be approximated by fuzzy logic Radhamohan et al. (2010), Sankaran (2008) or neural network (Kouda et al., 2002). An impulse momentum approach is included under energy based methods (Albahkali, 2011). Any energy based swing up methods can be heuristic to swing up the pendulum in short period of time (Wang, 2011; Christensen & Chistiansen, 2017). The other method is to consider closed loop fundamentals of the system, like frequency and damping coefficient (Donner et al., 2015).

In this paper, adaptive feedback linearization based controller is used for the stabilization of a pendulum on a cart at it's inverted position, by swinging the pendulum from it's pendant position using an adaptive fuzzy logic based swing up controller. The switching is performed using angle criteria.

2 System Design and Analysis

The dynamic equation of an inverted pendulum on a cart with mass of a cart m_c, mass of a pendulum m_p, arm length of a pendulum l and rotational inertia of a pendulum $I = 0.5m_pl^2$

shown on Figure 1 is given as,

$$\begin{aligned}\dot{x}_1 &= x_2 \\ \dot{x}_2 &= \frac{a}{c} + \frac{\xi}{c}u \\ \dot{x}_3 &= x_4 \\ \dot{x}_4 &= \frac{b}{c} + \frac{\eta}{c}u \end{aligned} \tag{1}$$

where

$$\begin{aligned} a &= (m_p l^2 + I) m_p l x_4^2 \sin x_3 - (m_p l)^2 g \sin x_3 \cos x_3 \\ b &= -(m_p l)^2 (x_4)^2 \sin x_3 \cos x_3 + (m_p + m_c) m_p l g \sin x_3 \\ c &= (m_p + m_c)(m_p l^2 + I) - (m_p l \cos x_3)^2 \\ \xi &= m_p l^2 + I \\ \eta &= -m_p l \cos x_3 \end{aligned}$$

2.1 Adaptive Feedback Linearization based Stabilizing Controller (AFLSC) Design

If the dynamics of an inverted pendulum is divided into cart subsystem and pendulum subsystem, the two subsystems fulfill integrability condition and involutivity condition. Cart subsystem:

$$\begin{aligned}\dot{x}_1 &= x_2 \\ \dot{x}_2 &= \frac{a}{c} + \frac{\xi}{c}u_1 \end{aligned} \tag{2}$$

Pendulum subsystem:

$$\begin{aligned}\dot{x}_3 &= x_4 \\ \dot{x}_4 &= \frac{b}{c} + \frac{\eta}{c}u_2 \end{aligned} \tag{3}$$

Input-state feedback linearizing control signals for the two subsystems are;

$$u_1 = \alpha_1^{-1}(x)(w_1 + \beta_1(x)) + u_{n1} \tag{4}$$

$$u_2 = \alpha_2^{-1}(x)(w_2 + \beta_2(x)) + u_{n2} \tag{5}$$

respectively. Where

$$\alpha_1(x) = \frac{\xi}{c}, \quad \alpha_2(x) = \frac{\eta}{c}, \quad \beta_1(x) = \frac{a}{c}, \quad \beta_2(x) = \frac{b}{c}$$

and

$$w_1 = -Fy + r_{poss} \quad and \quad w_2 = -Fy + r_{ang}$$

with this feedback linearization inputs signals the dynamic equation of each subsystem becomes,

$$\dot{y}_1 = y_2 \qquad \dot{y}_2 = w_1 \tag{6}$$

for cart subsystem and

$$\dot{y}_1 = y_2 \qquad \dot{y}_2 = w_2 \tag{7}$$

for pendulum subsystem. w_1 and w_2 are control signals for simplified subsystems. These control signals can be determined using any state feedback controller design methods. In this paper they are determined using linear quadratic regulator (LQR) controller design method on MATLAB. y_1 and y_2 are state variable of simplified subsystems. u_{n1}, and u_{n2}, are design signals that ensure robustness with respect to bounded error. While $r_{poss} = 0\ m$ and $r_{ang} = 0\ rad$ are reference position and reference angle respectively for the simplified subsystems.

The derivation of adaptive inverse control law and control signal is explained in (Tao, 2003). It suitable for nonlinear system with zero dynamics. Applying this method to inverted pendulum dynamics result in the following non-linearity signals $\omega_1(t)$ and $\omega_2(t)$ and unknown parameters θ_1 and θ_2 to be determined.

$$\omega_1(t) = \begin{bmatrix} w_1 \\ -w_1 \cos^2 x_3 \\ -x_4^2 \sin x_3 \\ \sin x_3 \cos x_3 \end{bmatrix},\ \omega_2(t) = \begin{bmatrix} w_2 \sec x_3 \\ -w_2 \cos x_3 \\ x_4^2 \sin x_3 \\ \tan x_3 \end{bmatrix}$$

$$\theta_1 = \begin{bmatrix} m_p + m_c \\ \frac{(m_p l)^2}{\xi} \\ m_p l \\ \frac{(m_p l)^2}{\xi} g \end{bmatrix}^T = \begin{bmatrix} \theta_{11} \\ \theta_{12} \\ \theta_{13} \\ \theta_{14} \end{bmatrix}^T, \theta_2 = \begin{bmatrix} \frac{m_p + m_c}{m_p l} \\ m_p l \\ m_p l \\ (m_p + m_c) g \end{bmatrix}^T = \begin{bmatrix} \theta_{21} \\ \theta_{22} \\ \theta_{23} \\ \theta_{24} \end{bmatrix}^T$$

The reference model for each subsystem is

$$\dot{y}_m = (A - Bk^*) y_m + Br \tag{8}$$

the tracking error is $\tilde{y} = y - y_m$ and choosing an adaptive law

$$\dot{\tilde{\theta}} = -\Gamma \omega(t) \tilde{y}^T(t) PB + f_\theta(t) \tag{9}$$

where $f_\theta(t)$ is called parameter projection function, which is defined as

$$f_\theta(t) = \begin{cases} 0 & if\ \theta_i \in [\theta_i^a, \theta_i^b]\ or \\ & if\ \theta_i = \theta_i^a\ and\ g_i(t) \geq 0\ or \\ & if\ \theta_i = \theta_i^b\ and\ g_i(t) \leq 0 \\ -g_i(t) & otherwise \end{cases} \tag{10}$$

$g_i(t)$ is given as;

$$g_i(t) = -\Gamma \omega(t) \tilde{x}^T PB \tag{11}$$

and $[\theta_i^a, \theta_i^b]$ is reasonable span of parameters, with θ_i^a minimum value and θ_i^b maximum value. While $\Gamma = diag[\gamma_1, \gamma_2, ..., \gamma_{n\theta}]$, and γ_i's are any positive real number for continuous time systems and $0 < \gamma_i < 2$ for discrete time systems. P is any positive definite matrix, $P = P^T > 0$ satisfying Lyapunov equation stated on equation 12.

$$P(A - Bk^*) + (A - Bk^*)^T P = -2Q \tag{12}$$

where, Q is any positive definite matrix, $Q = Q^T > 0$.
Taking Lyapunov function

$$\nu(\tilde{x}, \tilde{\theta}) = \frac{1}{2}(\tilde{y}^T P \tilde{y} + \tilde{\theta}^T \Gamma^{-1} \tilde{\theta}) \tag{13}$$

The derivative of Lyapunov function is

$$\dot{\nu} = \tilde{y}^T P \dot{\tilde{y}} + \tilde{\theta}^T \Gamma^{-1} \dot{\tilde{\theta}} \tag{14}$$

If disturbance $d_N(t) = 0$, select design signal $u_n = 0$ and parameter projection function $f_\theta(t) = 0$. With an adaptive law on equation (9),

$$\tilde{y}^T PB\tilde{\theta}^T\omega + \tilde{\theta}^T\Gamma^{-1}\dot{\tilde{\theta}} = 0 \tag{15}$$

Which means the derivative of lyapunov function

$$\dot{\nu} = -\tilde{y}^T Q\tilde{y} \leq 0 \tag{16}$$

as desired. This means that ν is bounded and $\tilde{y} = y - y_m \in L^2$ ı.e $\tilde{y}$ and $\tilde{\theta}$ are bounded, so are y and θ. Since $\dot{y} = T(x)$ is diffeomorphism, $x(t)$ is also bounded and so are u_d and $\dot{\tilde{y}}$, which implies $\lim_{t\mapsto 0}(y(t) - y_m(t)) = 0$. If disturbance $d_N(t) \neq 0$ choose design signal

$$u_n = -\gamma\alpha(x)\tilde{y}^T PB \tag{17}$$

where γ is any positive real number. Under this condition the derivative of lyapunov function becomes,

$$\dot{\nu} = -\tilde{y}^T Q\tilde{y} + \tilde{\theta}^T\Gamma^{-1} f_\theta + \frac{1}{4\gamma}d_N^2 \tag{18}$$

Since $d_N(t)$ is bounded, $\tilde{y}$ is bounded so is $y(t)$. Then $x(t)$ is bounded, because $T(x)$ is diffeomorphism and $u_d(t)$ is also bounded.

2.2 Adaptive Fuzzy Logic based Swing-up Controller (AFLSUC) Design

Swinging the pendulum from pendant position can be achieved by many different methods. From those methods this paper uses impulse-momentum swing up approach approximated by fuzzy logic. An impulse-momentum approach can be used with other stabilizing controllers (Albahkali, 2011). The designed adaptive fuzzy logic based swing-up controller has two inputs and one output. The inputs are cart position error ex_1 (deviation from $x = 0$) and angular position error ex_3 (deviation from $\theta = \pi$). The output is control signal u. Each input signals have three membership functions, namely Negative (N), Zero (Z) and Positive (P). while output control signal has five membership functions, namely Negative Big (NB), Negative Small (NS), Zero (Z), Positive Small (PS) and Positive Big (PB). Fuzzy logic rule base of the designed controller is shown on Table 1. Membership functions of inputs (linear position error and

Table 1: Fuzzy Rule base for swing-up

$ex_1 \setminus ex_3$	N	Z	P
N	PB	Z	PS
Z	NS	Z	PS
P	NB	Z	NS

angular position error)to fuzzy logic based swing up controller are indicated on Figure 2 and Figure 3 respectively.

The output control signal membership function of fuzzy logic based swing up controller is shown on Figure 4. This controller can be made adaptive for smaller range of cart mass and pendulum mass. The adaption mechanism for fuzzy logic based swing up controller is derived from the change in mechanical energy of the pendulum. Taking the reference mechanical energy of the pendulum to be $m_p gl$. The change in mechanical energy of a pendulum is

$$\begin{aligned}\dot{E}_p &= \frac{d}{dt}\left(0.5(m_p l^2 + I)\dot{\theta}^2 + m_p gl(1 + \cos\theta)\right)\\ \dot{E}_p &= -m_p l\dot{\theta}\cos\theta\end{aligned} \tag{19}$$

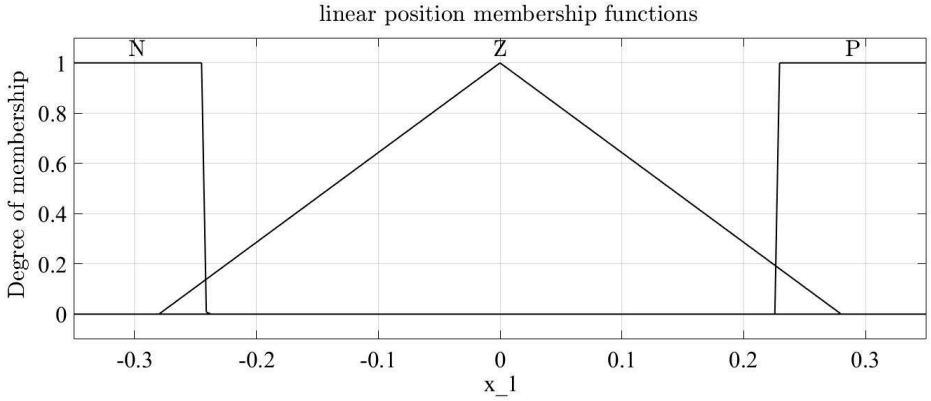

Figure 2: Cart linear position membership function

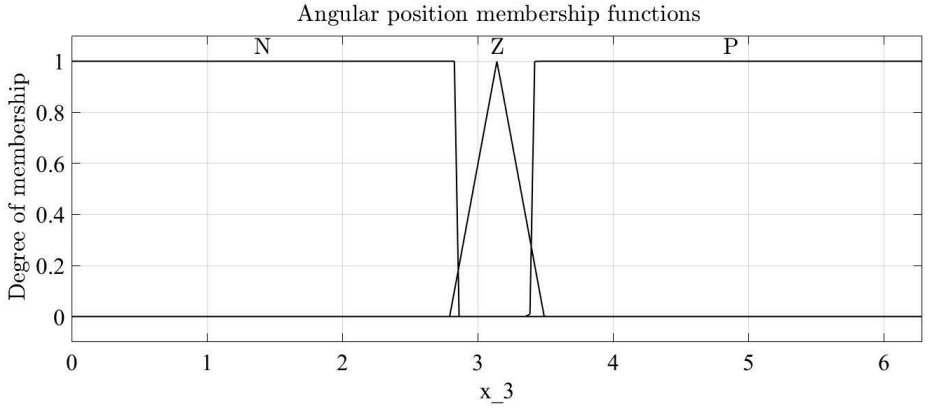

Figure 3: Pendulum angular position membership functions

From equation 19 the variables m_p and l are unknown the only way to alter the energy of the system is by changing angular velocity $\dot{\theta}$ or angle θ. But, maximum energy is injected to the system or removed from system when it's angular position is zero (when the pendulum crosses a vertical line joining the two equilibrium points $(0, 0, 0, 0)$ and $(0, 0, \pi, 0)$). The change in angular velocity of the pendulum can infer the amount of energy injected to the system or removed from the system. Thus this can be used to adjust the amount of energy injected to the system. By applying this method, the pendulum can be driven from pendant position to upright or inverted position in less than 2 seconds.

The mass of the cart has significant effect on the amount of energy injected to the system. In this paper the scalar multiplier for an adaptive fuzzy logic based swing-up controller output signal is selected manually for particular initial mass of a cart.

2.3 Switching Condition

Switching takeoff between AFLSUC and AFLSC when the pendulum reach in region $\left(-\pi + \frac{\pi}{9}, \pi - \frac{\pi}{9}\right)$.

3 Simulation Result

3.1 Phase Portraits of IPC Natural Dynamics

Phase plane analysis is powerful tool in analysis of non linear system behavior as indicated on (Slotine & Li, 1991). The simulation of inverted pendulum dynamics is analyzed using this

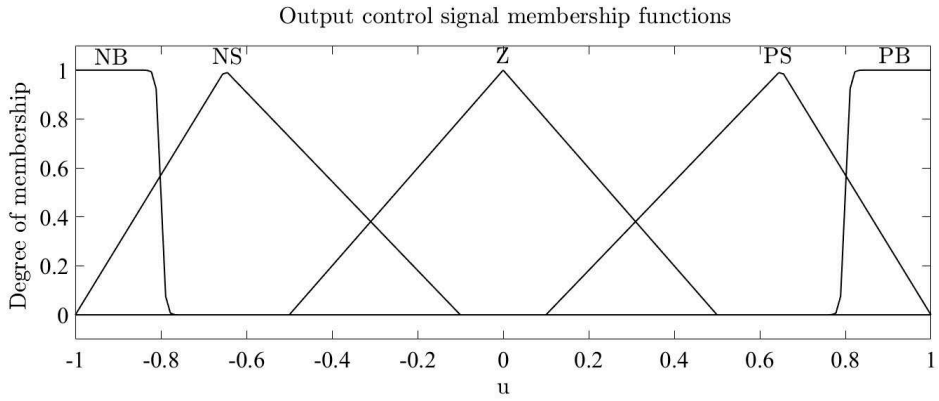

Figure 4: Control signal membership function

method. The simulation of cart subsystem dynamics and pendulum subsystem dynamics of IPC with out controller are shown on Figure 5 and 6 respectively. The position subsystem has stable focus at $(x, 0)$. Linear position is a free variable ı.e the equilibrium point of linear position can be anywhere as seen from Figure 5, which in this case x_{eq} is taken to be 0. Similarly the angle subsystem has stable focus at $(0, 0)$ as indicated on Figure 6.

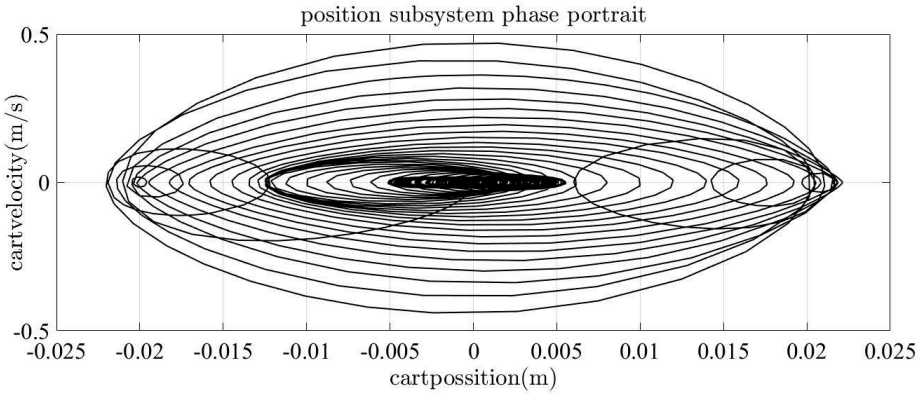

Figure 5: Cart subsystem natural dynamics phase portrait

3.2 Response of the System with AFLSC

The performance of the controller depends design parameters as shown on Tao (2003). For some design parameters the dynamics of IPC doesn't converge ı.e the dynamics of IPC becomes uncontrollable.

In this paper the design parameters are selected manually by looking at the response of the response of IPC on MATLAB/SIMULINK simulation. From these observations, very large element values of Q matrix makes the dynamics of IPC uncontrollable. For very small element values for Q matrix the position of the cart becomes out of range. The summary of this observation is shown on Table 2.

In this paper the value of Q matrix is selected to be;

$$Q = \begin{bmatrix} 0.0045 & 0.0030 \\ 0.0030 & 0.0045 \end{bmatrix}$$

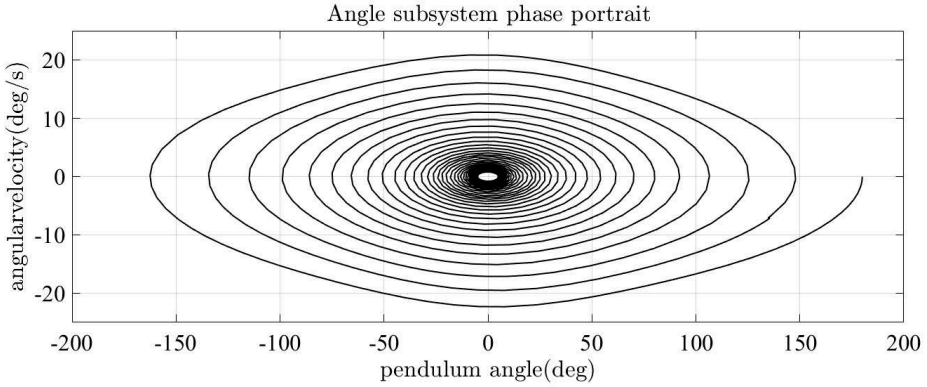

Figure 6: Pendulum subsystem natural dynamics phase portrait

Table 2: Q matrix selection range

values	x_1 response	x_3 response
< 0.001	out of range	smaller settling time
≥ 0.001 and < 0.1	within range	small settling time
≥ 0.01	uncontrollable	uncontrollable

The other design parameters are selected by similar way. For cart subsystem $\gamma = 240$ and $\gamma = 12$ for pendulum subsystem. While

$$\Gamma = \begin{bmatrix} 0.5 & 0 & 0 & 0 \\ 0 & 0.5 & 0 & 0 \\ 0 & 0 & 0.5 & 0 \\ 0 & 0 & 0 & 0.5 \end{bmatrix}$$

for both subsystems and finally $\sigma = 250$.

The initial conditions, minimum and maximum value of system parameters and physical constraints for simulation are listed in Table 3 and Table 4 respectively.

Table 3: Range of system parameters

parameter	init. value	min. value	max. value
mass of cart	0.1 kg	0.02 kg	4 kg
mass of pend.	0.01 kg	0.002 kg	4 kg
length of pend.	0.1 m	0.1 m	1 m

3.3 IPC Phase Portraits with AFLSC

Figure 7 shows the phase portrait of the system with AFLSC for cart subsystem with different values of m_p under constant value of m_c. Figure 9 show cart subsystem phase portrait with AFLSC for different values of m_c with constant value of m_p. Figure 8 shows phase portraits of pendulum subsystem with AFLSC for different values of m_p with constant value of m_c. Where as Figure 10 shows phase portraits of pendulum subsystem with AFLSC for different values of m_c with constant value of m_p. From this results, it can be concluded that the controller changes the unstable saddle equilibrium point $(0, 0, \pi, 0)$ to stable focus for different values of m_c and m_p in the range shown on Table 3.

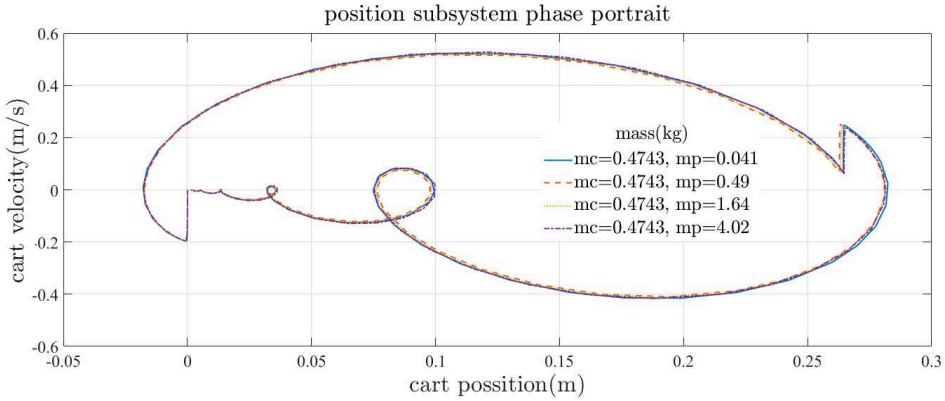

Figure 7: Cart subsystem phase portraits with different values of m_p

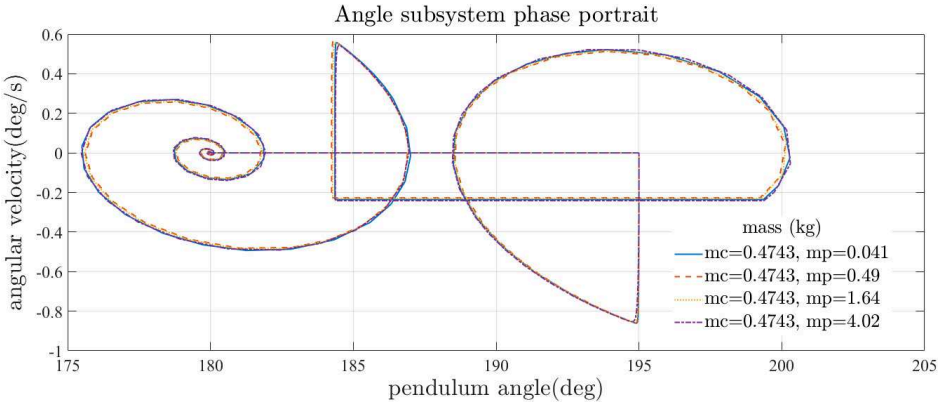

Figure 8: Pendulum subsystem phase portraits with different values of m_p

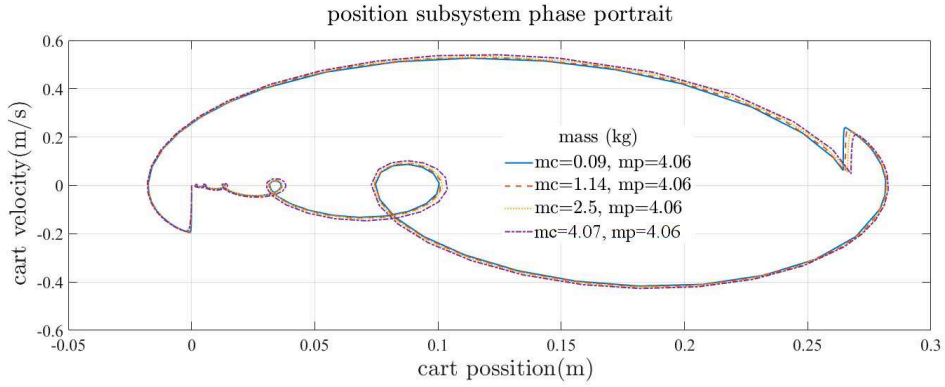

Figure 9: Cart subsystem phase portraits with different values of m_c

Table 4: Physical constraints

parameter	value
linear friction coefficient	0.1 N/m
angular friction coefficient	0 rad/s
linear damping coefficient	0.01 N/(m/s)
angular damping coefficient	0.00025 rad/(m/s)
gravitational acceleration	9.81 m/s^2

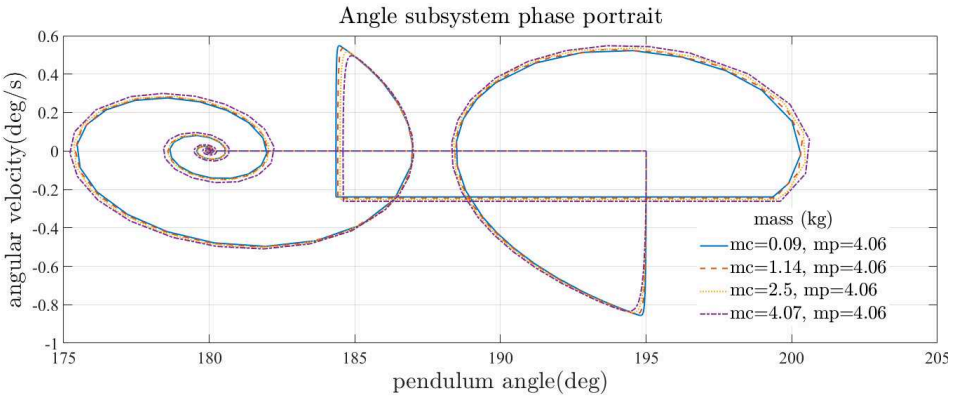

Figure 10: Pendulum subsystem phase portraits with different values of m_c

3.4 Response of the System with AFLSC and AFLSUC

The cart subsystem phase portraits of the combined controller for different value of m_p are shown on Figure 11 and Figure 13 for fuzzy logic controller output gain multiplier $k = 6$ and $k = 12$ respectively. The respective pendulum subsystem phase portraits are shown on Figure 12 and Figure 14. For different value of m_c the cart subsystem phase portraits are shown on Figure 15 for $k = 6$ and Figure 17 for $k = 12$. The respective pendulum subsystem phase portraits under different m_c are shown on Figure 16 and Figure 18.

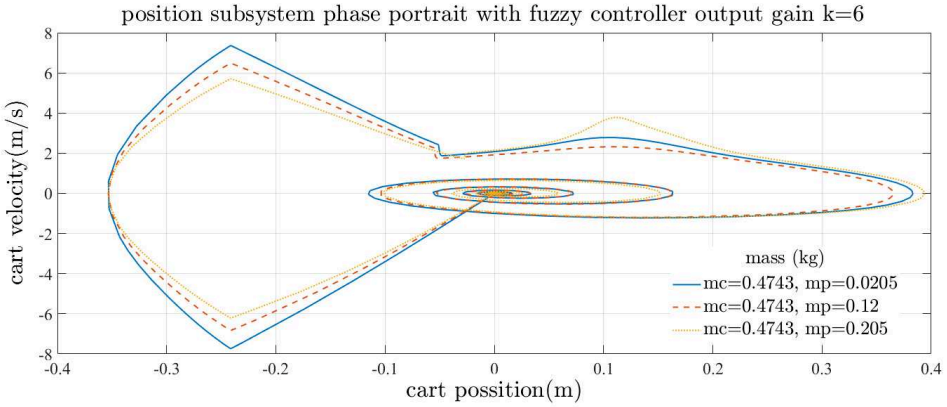

Figure 11: Cart subsystem phase portraits with different values of m_p for $k = 6$

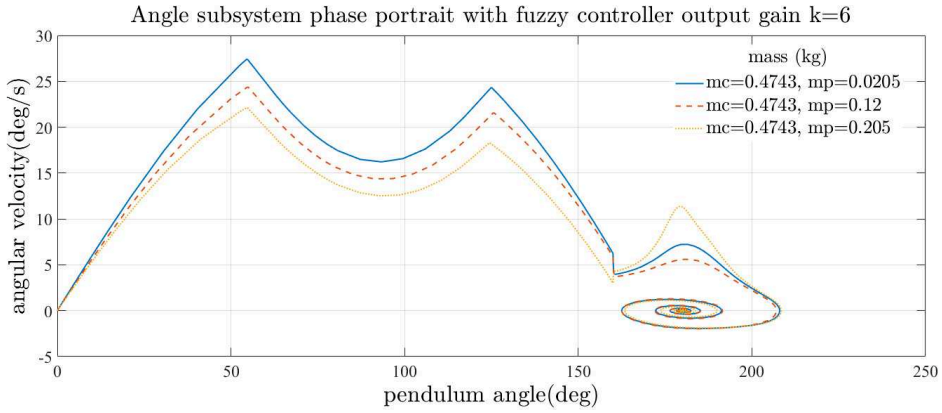

Figure 12: Pendulum subsystem phase portraits with different values of m_p for $k = 6$

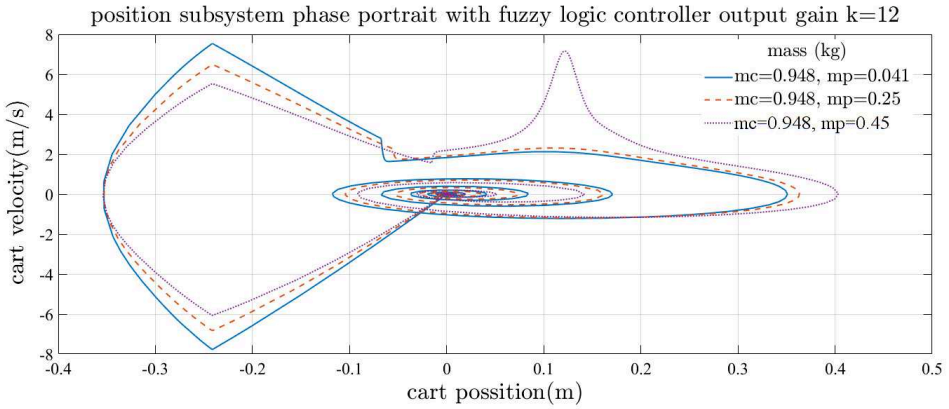

Figure 13: Cart subsystem phase portraits with different values of m_p for $k = 12$

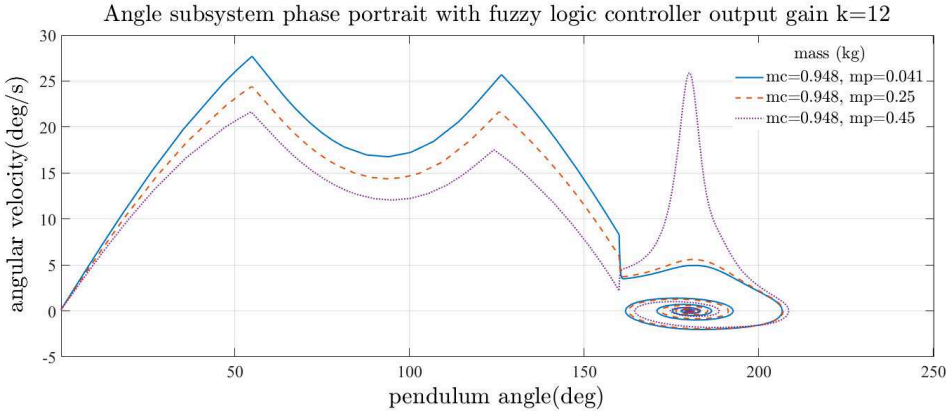

Figure 14: Pendulum subsystem phase portraits with different values of m_p for $k = 12$

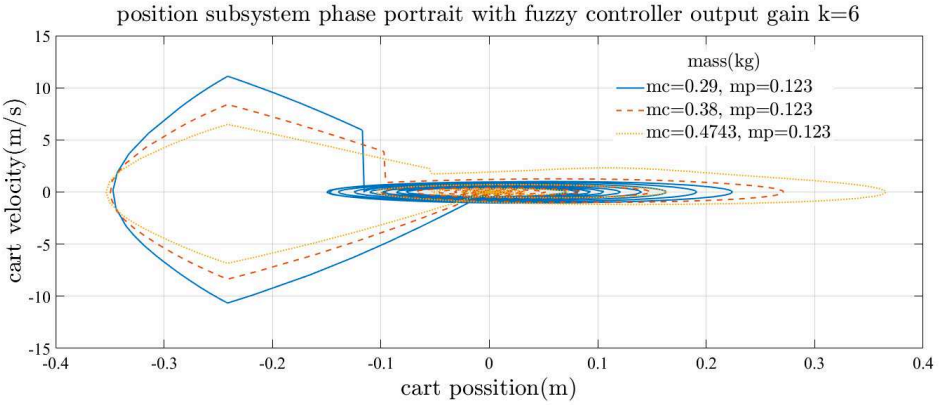

Figure 15: Cart subsystem phase portraits with different values of m_c for $k = 6$

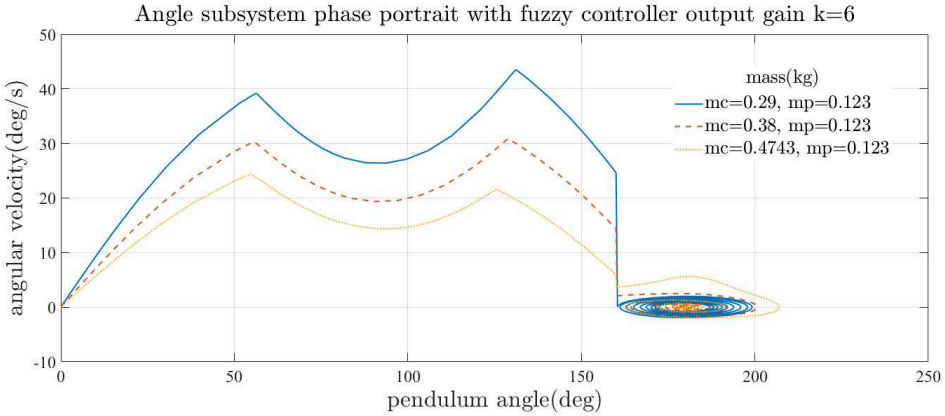

Figure 16: Pendulum subsystem phase portraits with different values of m_c for $k = 6$

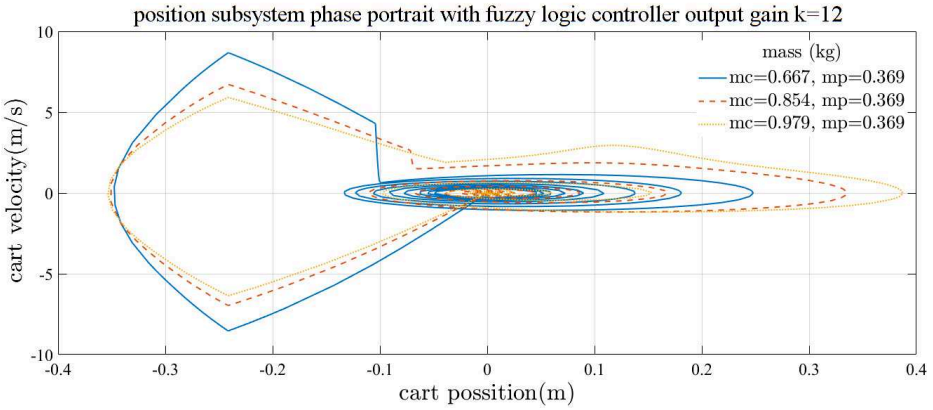

Figure 17: Cart subsystem phase portraits with different values of m_c for $k = 12$

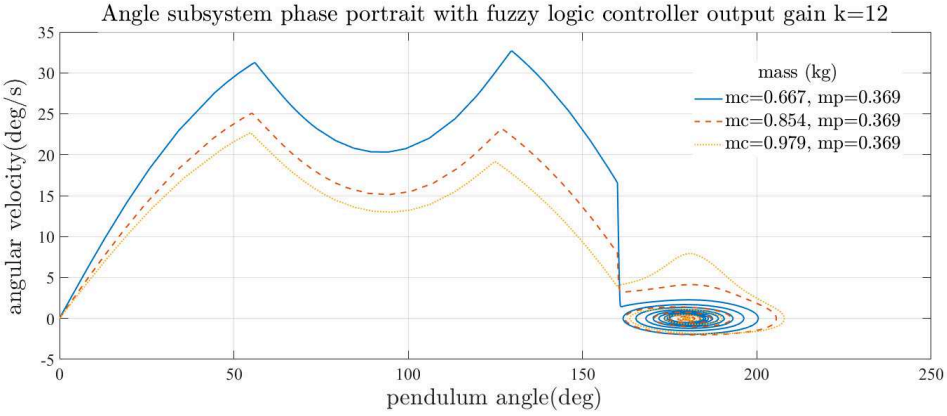

Figure 18: Pendulum subsystem phase portraits with different values of m_c for $k = 12$

These phase portraits shows that the controllers changes the unstable equilibrium point$(0, 0, \pi, 0)$ to stable focus. The peaks that appear near $(0, 0, \pi, 0)$ on the phase portraits shows incapability of AFLSUC in driving the pendulum from pendant position to vicinity of its inverted position without changing the controller's output multiplier gain k. This due to the reason that AFLSUC is unable to adapt to the whole range of system parameters shown on Table 3.

4 Integrated Hardware Setup Description

The laboratory in Figure 20 setup is prepared from printing old machine. It is arranged and developed in such a way that it suits for this application with the help of Mechanical and Industrial engineering department of laboratory. The hardware setup consists of a pendulum

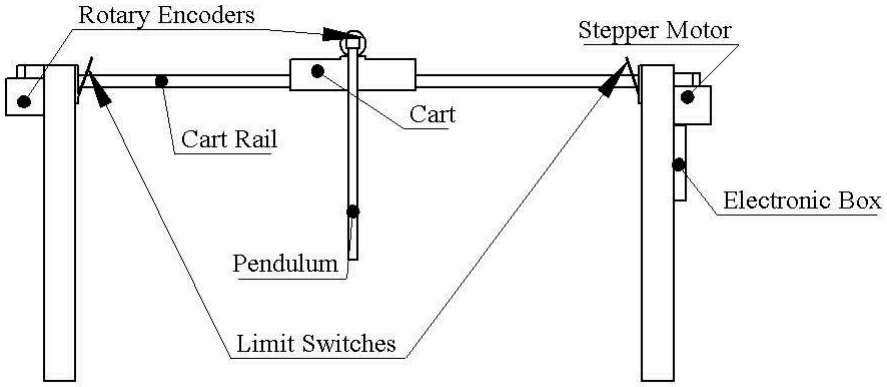

Figure 19: Integrated system hardware setup

attached to a cart. The cart is attached to the rail, and is able to move horizontally. A belt connects the cart to the pulleys at each end of the rail. The pulley at the right side is mounted on shaft of stepper motor, which effectively drives the cart. The pulley on the other end is mounted on shaft of incremental rotary encoder. This incremental rotary encoder measure the cart position.

The incremental rotary encoder used in this thesis hardware experimentation has a resolution of 400 pulse per revolution(PPR). Which shows that the total pulse generated for both channel of the encoder is 1600 pulses.

To determine the linear position of the cart the number of pulses generated over maximum rail length is counted first. The maximum rail length is $0.85m$ then for any count the conversion to rail length in meters m is

$$x_1 = \frac{pulse\ counted}{pulse\ counted\ for\ l_{rmax}} l_{rmax}$$

where l_{rmax} is maximum rail length.

The pendulum consists of a light metal rod attached to incremental optical rotary encoder,which is used to measure the angular displacement of the pendulum and angular velocity of the pendulum. The angular position of the pendulum is determined as,

$$x_3 = 2\pi \frac{Number\ of\ pulse\ counted}{1600}$$

Linear velocity of the cart and angular velocity of the pendulum are taken as time derivative of cart position and angular position of the pendulum respectively.

The Electronic box on Figure 19 symbolises the electronics of the setup, which includes stepper motor, motor driver, an Arduino and power supply unit. The two incremental rotary encoder are connected to arduino hardware interrupt pins. Arduino Mega2560 is suitable for this hardware experimentation, as it has six pins to read external interrupts.

Figure 20: Hardware setup for Experimentation

The code for AFLSC is changed in a way that it is suitable for implementation on arduino to test the performance of the controller. Thus arduino can process the computation standalone. But since the result of the hardware experimentation is required the data is sent to laptop to analyze it using virtual oscilloscope. The virtual oscilloscope is called Serialplot[1]. Regarding AFLSUC the computation on MATLAB/SIMULINK is possible, but adapting the controller code to arduino code was unsuccessful.

A DC voltage source of magnitude $12V$ is applied to the stepper motor. There are two mechanical toggle switches at each end of the rail, when the cart reaches at these positions it

[1]Serialplot is a free software to plot and analyze data from serial port, which can be downloaded from https://hackaday.io/project/5334-serialplot-realtime-plotting-software

switch off the voltage source. It is possible to monitor it using soft-computation but, if the cart it at high speed it is not possible to stop it. The encoder need a DC voltage source of magnitude $5V$ to operate, which ca be supplied from arduino Mega2560 board. To read the count of the encoders, encoder library (Encoder.h[2]) is used. While for stepper motor control internal arduino library is used. The overall block diagram representation of the system is shown on Figure 21. The control command applied to the stepper motor is position control command.

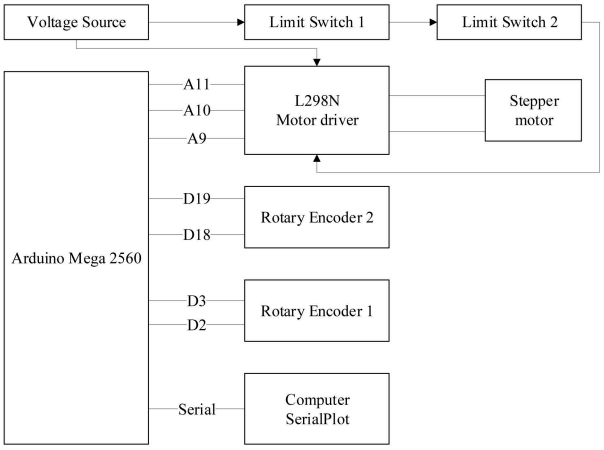

Figure 21: Electrical circuit block diagram representation

The pendulum is driven to it's inverted position manually. When the pendulum reaches in the range $(\pi - \frac{\pi}{9}, \pi + \frac{\pi}{9})$ AFLSC will be switched on to stabilize the pendulum at its unstable point.

5 Experimentation Result

5.1 Hardware setup validation

Before testing AFLSC the validation of the developed hardware is tested. The result of the angular position of the pendulum under no control action is shown on Figure 22 and response of the cart position is shown on Figure 23. The angular friction of rotary encoder is negligible, which can be inferred from the Figure

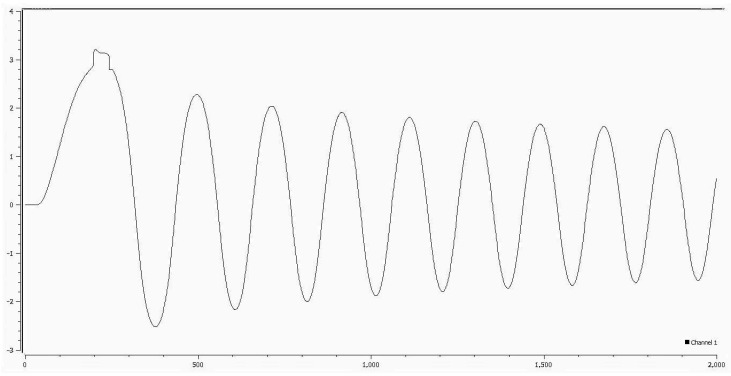

Figure 22: Pendulum angular position natural dynamics

Linear bearing is used to minimize the friction between the cart and the rail. But still the friction is significant. This can be understood from the position response of the cart. If it was

[2]Encoder.h library is downloaded from https://www.arduinolibraries.info/libraries/encoder

small the cart angular position response will look like sinusoidal wave form as on on Figure22. Since the controller is adaptive it should have overcome this problem, and it does.

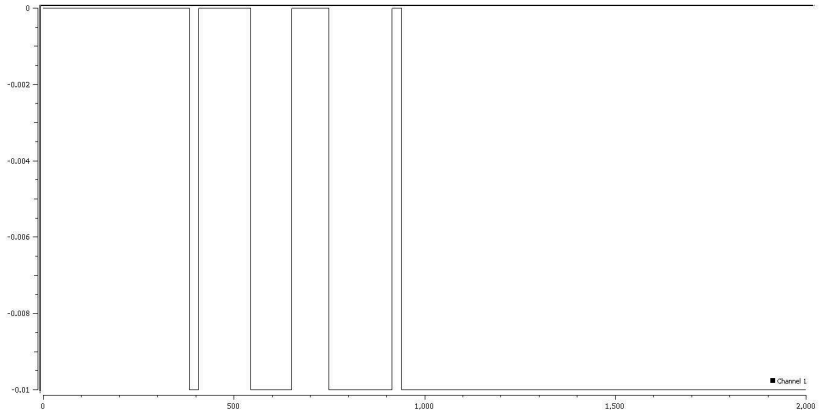

Figure 23: Cart position natural dynamics

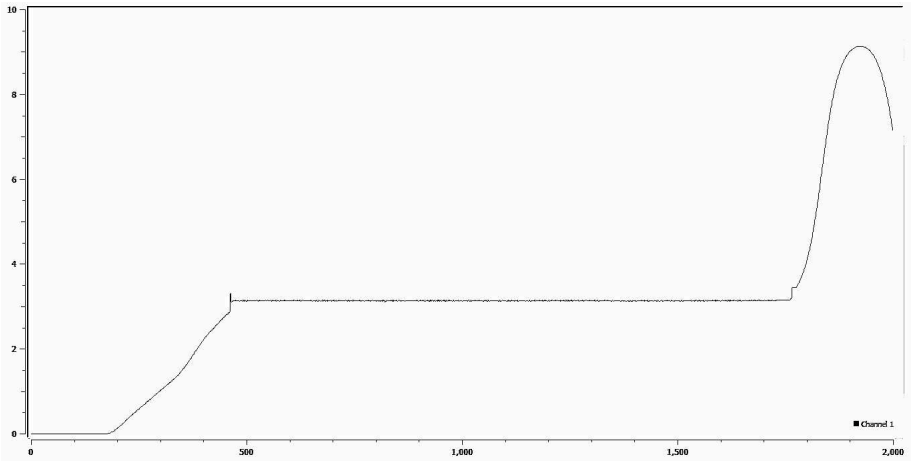

Figure 24: Pendulum angular position response with AFLSC

The position of the cart with AFLSC is shown on Figure 25. This result depict the same scenario.

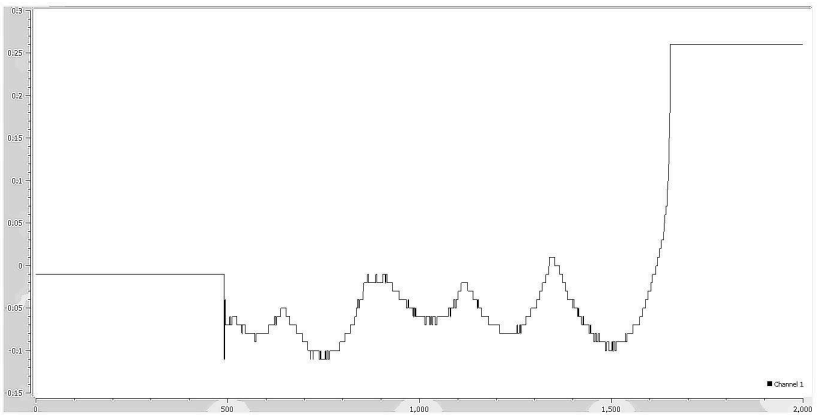

Figure 25: Cart position response with AFLSC

5.2 Response of the hardware setup with AFLSC

The response of the angular position of the pendulum with AFLSC is shown on Figure 24. The controller stabilize the pendulum. But as time goes on the defect in mechanical design force the pendulum to fall. This defect is caused by the misalignment of the pendulum center of mass and the cart center of mass. Thus when the pendulum moves large angel in one direction the controller is unable to respond at required rate, because the pendulum falls at high rate. Figure24 shows the same result.

6 Conclusion

This paper introduced application of feedback linearization to inverted pendulum on a cart stabilization problem and adaptive fuzzy swing up to swing up problem of a pendulum. By decomposing the system into cart subsystem and pendulum subsystem in combination with adaptive inverse control to stabilize a pendulum about upright position. While AFLSUC is used to swing up a pendulum from it's pendant position to inverted position. Simulation result shows promising result under different cart mass and pendulum mass for $0.3m - 0.4m$ arm length pendulum. For disturbance up to ± 15 degree an AFLSC stabilize the system with small deviation in the position of the cart from origin $(0, 0)$.

Combining AFLSC with AFLSUC maximum deviation of the cart position from origin $(0, 0)$ is $0.35m$. The combined controller have adapted to 4 initial mass of the cart and 10 times initial mass of the pendulum after selecting fuzzy logic controller output gain multiplier.

The hardware experimentation shows promising result under unknown cart mass and pendulum mass. Additionally the arm length of the pendulum used in hardware experimentation is unknown. Thus the simulation results and hardware experimentation results shows that an AFLSC is a solution to stability problem of an arbitrary inverted pendulum on a cart. While from simulation results it can be concluded that an AFLSUC is a solution for swing up problem of an arbitrary pendulum from it's pendant position.

References

Albahkali, T.A. (2011). An Impulse-Momentum Approach to Swing-Up Control of Double Inverted Pendulum on a Cart. World Academy of Science, Engineering and Technology, 54.

Åström, K.J., Furuta, K. (2000). Swinging up a pendulum by energy control. *Automatica, 36*(2), 287-295.

Chanchareon, R., Sangveraphunsiri, V., & Chantranuwathana, S. (2006, June). Tracking control of an inverted pendulum using computed feedback linearization technique. In *2006 IEEE Conference on Robotics, Automation and Mechatronics* (pp. 1-6). IEEE.

Chen, C.S., Chen, W.L. (1998). Robust adaptive sliding-mode control using fuzzy modeling for an inverted-pendulum system. *IEEE Transactions on Industrial Electronics, 45*(2), 297-306.

Christensen, J.H., & Chistiansen, R. (2017). Swing Up and Stabilisation of an Inverted Pendulum on a Cart using Nonlinear Methods. Unpublished master theses. Aalborg East: Aalborg University.

Donner, P., Christange, F., & Buss, M. (2015, July). Adaptive simple pendulum swing-up controller based on the closed-loop fundamental dynamics. In *2015 European Control Conference* (ECC) (pp. 2798-2805). IEEE.

El-Hawwary, M.I., Elshafei, A.L., Emara, H.M., & Fattah, H.A.A. (2006). Adaptive fuzzy control of the inverted pendulum problem. *IEEE Transactions on Control Systems Technology, 14*(6), 1135-1144.

Garcia-Chavez, G., Munoz-Panduro, E. (2017, August). Global control for the Furuta Pendulum based on Partial Feedback Linearization and stabilization of the Zero Dynamics. In *2017 13th IEEE Conference on Automation Science and Engineering* (CASE) (pp. 334-339). IEEE.

James, A.A. (2015). Feedback linearization, sliding mode and swing up control for the inverted pendulum on a cart. M.S. thesis, University of Manchester, Faculty of Engineering and Physical Sciences.

Jeon, S.H., Choi, J.Y. (2000, July). Adaptive feedback linearization control based on stator flux model for induction motors. In Proceedings of the 2000 *IEEE International Symposium on Intelligent Control. Held jointly with the 8th IEEE Mediterranean Conference on Control and Automation* (Cat. No. 00CH37147) (pp. 273-278). IEEE.

Kouda, N., Matsui, N., & Nishimura, H. (2002, August). Control for swing-up of an inverted pendulum using qubit neural network. In *Proceedings of the 41st SICE Annual Conference. SICE 2002.* (Vol. 2, pp. 765-770). IEEE.

Mladenov, V., Tsenov, G., Ekonomou, L., Harkiolakis, N., & Karampelas, P. (2009, May). Neural network control of an inverted pendulum on a cart. In *WSEAS International Conference. Proceedings. Mathematics and Computers in Science and Engineering* (No. 9). World Scientific and Engineering Academy and Society.

Ogata, K., Yang, Y. (2002). *Modern Control Engineering.* Prentice-Hall, vol. 4.

Park, M.S., Chwa, D. (2009). Swing-up and stabilization control of inverted-pendulum systems via coupled sliding-mode control method. *IEEE transactions on industrial electronics, 56*(9), 3541-3555.

Pathak, K., Franch, J., & Agrawal, S.K. (2005). Velocity and position control of a wheeled inverted pendulum by partial feedback linearization. *IEEE Transactions on robotics, 21*(3), 505-513.

Radhamohan, S.V., Subramaniam, M.O.N.A., & Nigam, M.J. (2010). Fuzzy swing-up and stabilization of real inverted pendulum using single rulebase. *Journal of Theoretical and Applied Information Technology, 14*(1/2), 43-49.

Renou, S., Saydy, L. (1996, May). Real time control of an inverted pendulum based on approximate linearization. In *Proceedings of 1996 Canadian Conference on Electrical and Computer Engineering* (Vol. 2, pp. 502-504). IEEE.

Shameli, E., Khamesee, M.B., & Huissoon, J.P. (2008, August). Application of a model reference adaptive feedback linearization controller to a magnetic telemanipulation system. In *2008 IEEE International Conference on Mechatronics and Automation* (pp. 219-223). IEEE.

Slotine, J.J.E., Li, W. (1991). *Applied Nonlinear Control* (Vol. 199, No. 1). Englewood Cliffs, NJ: Prentice hall.

Tao, C.W., Taur, J.S., Hsieh, T.W., & Tsai, C.L. (2008). Design of a fuzzy controller with fuzzy swing-up and parallel distributed pole assignment schemes for an inverted pendulum and cart system. *IEEE Transactions on Control Systems Technology, 16*(6), 1277-1288.

Tao, G. (2003). *Adaptive Control Design and Analysis* (Vol. 37). John Wiley & Sons.

Torres, L.H., Schnitman, L., Junior, C.A.V.V., & de Souza, J.F. (2012). Feedback linearization and model reference adaptive control of a magnetic levitation system. *Studies in Informatics and Control, 21*(1), 67-74.

Wang, Y. (2016). Optimal swing-up control of an inverted pendulum.

Wu, J., Wang, Z. (2011, October). Research on fuzzy control of inverted pendulum. In *2011 First International Conference on Instrumentation, Measurement, Computer, Communication and Control* (pp. 868-871). IEEE.

Yakoub, Z., Charfeddine, M., Jouili, K., & Braiek, N.B. (2013, March). A combination of backstepping and the feedback linearization for the controller of inverted pendulum. In *10th International Multi-Conferences on Systems, Signals & Devices 2013* (SSD13) (pp. 1-6). IEEE.

Yoshida, K. (1999, June). Swing-up control of an inverted pendulum by energy-based methods. In *Proceedings of the 1999 American Control Conference* (Cat. No. 99CH36251) (Vol. 6, pp. 4045-4047). IEEE.